Available online at www.sciencedirect.com
SCIENCE DIRECT
Catalysis Today 116 (2006) 415–421
CATALYSIS TODAY
www.elsevier.com/locate/cattod

CO tolerant catalysts for PEM fuel cells Spectroelectrochemical studies

G. García [a], J.A. Silva-Chong [a], O. Guillén-Villafuerte [a], J.L. Rodríguez [a], E.R. González [b], E. Pastor [a,*]

[a] *Departamento de Química Física, Universidad de La Laguna, 38071 Tenerife, España, Spain*
[b] *Instituto de Química de São Carlos, USP, C.P. São Carlos, SP 13560-970, Brazil*

Available online 7 July 2006

Abstract

CO tolerance of carbon-supported $Pt_{80}Ru_{20}$, $Pt_{80}Os_{20}$ and $Pt_{85}Co_{15}$ electrocatalysts has been studied in 0.1 M perchloric acid solution applying cyclic voltammetry and in situ Fourier transform infrared spectroscopy (FTIRS), and the results were compared with those for a commercial Pt ETEK catalyst. CO stripping is used for the normalization of the area of the electrodes. It is shown that FTIR spectra can be acquired during CO oxidation at these technical materials in an electrochemical cell, obtaining valuable information on the reactivity, which allows predicting their behaviour in a polymer electrolyte membrane fuel cell (PEMFC). Linear adsorbed CO is the main adsorbate, but also small amounts of bridge bonded CO are formed. Moreover, COH species seem to be also present for $Pt_{80}Os_{20}$ and $Pt_{85}Co_{15}$. On the other hand, the onset potential for CO oxidation to CO_2 is established and compared for the four catalysts. All bimetallic alloys are able to oxidise adsorbed CO at lower potentials than platinum and a shift of about 0.20 V is determined.

Keywords: Bimetallic Pt alloys; Carbon-supported catalysts; In situ FTIRS; Cyclic voltammetry; CO tolerance

1. Introduction

Research on alternatives to hydrogen as a fuel has been focused on the oxidation of small organic molecules and, considering the current state of the development, the use of methanol has been established as the better alternative. Direct methanol fuel cells (DMFCs) are attractive devices to convert chemical energy into electric energy, but their performance is limited by various problems, including kinetic restraints and methanol cross-over from the anode to the cathode side through the membrane [1]. Moreover, the use of hydrogen obtained from reforming of other fuels is a convenient economic alternative to pure hydrogen. However, both options have the drawback of the continuous poisoning of the catalysts due the presence of CO as impurity generated in the reforming process or as intermediate formed in the dissociative adsorption of methanol on the catalyst (usually Pt). One of the most important research activities nowadays is the study of CO electrooxidation and the development of electrode materials that are more tolerant to the presence of small amounts of CO.

In fact, in order to understand the kinetic and mechanism of fuel cell reactions, anode catalysts which combine a high activity for methanol dehydrogenation and an improved tolerance towards CO poisoning are required [1].

At present, it is accepted that Pt–Ru alloys are the most active electrocatalysts for methanol oxidation. Otherwise, the improvement of the CO electrocatalysis has been ascribed to different factors such as changes in the Pt–Pt interatomic distance [2], the composition of the alloy [3], the surface area [4] and the Pt electronic configuration [5].

Several approaches have been used for the production of catalysts both supported and unsupported. Reduction of the metallic ions from their salts with sulphite [6], borohydride [7], formaldehyde [8], hydrazine [9] or formic acid [10,11] has been proposed, resulting in catalysts with such diverse physical characteristics that direct comparison of their electrochemical performances is a rather difficult task. In the case of bimetallic catalysts, the reduction of both metals can be done simultaneously or one after the other, as it was described for Pt–Ru/C [12] and Pt–Co/C [13].

* Corresponding author. Fax: +34 922 318 002.
E-mail address: epastor@ull.es (E. Pastor).

0920-5861/$ – see front matter © 2006 Elsevier B.V. All rights reserved.
doi:10.1016/j.cattod.2006.05.069

The optimum particle size for methanol oxidation has been the subject of several investigations and the values vary with the preparation procedure, the conditions of the reaction and the metals present in the catalyst. It has been found that the optimum specific activity for Pt was achieved with particle sizes of 3 nm [14]. Other reports [15,16] conclude that the specific activity declines below 4.5 nm. Particles below 5.0 nm have enough coordination sites to produce strong Pt–OH bonds leading to high coverages with this species.

Mukerjee and McBreen have studied the role of the geometric parameters and the changes in the electronic structure due to specific adsorbates, such as hydrogen and oxygenated species (OH and CO), on methanol oxidation [17]. They found by X-ray absorption spectroscopy that, for particle sizes of carbon-supported Pt clusters below 5.0 nm, there is a strong adsorption of H, OH and C_1-compounds such as CO. On these small particles, H adsorption is strong enough to induce restructuring and morphological changes in Pt clusters at negative potentials. Moreover, the strong adsorption of OH for potentials more positive than 0.8 V inhibits the reduction of oxygen, and the combined effect of strongly adsorbed CO and OH impedes the oxidation of methanol.

In order to understand the mechanism of CO and methanol electrooxidation on binary platinum alloys catalysts, much work is needed on the surface structure (including electronic aspects) and its relationship with the reactivity. Adsorbed carbon monoxide exhibits a surface sensitive behaviour which influences the vibrational frequencies of the C–O band. Consequently, in situ Fourier transform infrared spectroscopy (FTIRS) appears to be a useful technique to study the CO interaction with the surface.

In this work, carbon-supported $Pt_{80}Ru_{20}$, $Pt_{80}Os_{20}$ and $Pt_{85}Co_{15}$ electrocatalysts were prepared by reduction with formic acid or sodium borohydride. At room temperature, PtRu alloys having a Ru content between 10 and 40% are the best catalysts for methanol oxidation [1]. Accordingly, a Pt:Ru atomic ratio in this range is selected for the present study and similar ratios are considered for the other alloys. Thus, results on the CO tolerance of these materials can be compared with those on the adsorption and oxidation of methanol. These studies are in progress and will be the subject of a forthcoming publication.

The spectroelectrochemical properties were compared with commercial Pt/C. Accordingly, we have undertaken a systematic investigation on the electrochemical behaviour of CO using conventional electrochemical methods combined with a spectroscopic in situ technique such as FTIRS. Using an appropriate experimental setup, the latter technique can be used to characterize submonolayers of adsorbate by means of the anodic stripping of the layer [18,19]. Finally, the nature of the adsorbed species and the oxidation products is discussed on the basis of the spectral data obtained at different potentials and compared with the electrochemical results.

2. Experimental

Carbon-supported $Pt_{80}Ru_{20}$ and $Pt_{80}Os_{20}$ electrocatalysts were prepared by chemical reduction with formic acid (Mallinkrodt AR®). This procedure is usually called formic acid method (FAM) [10,20,21]. On the other hand, carbon-supported $Pt_{85}Co_{15}$ was prepared by reduction of the ionic precursors (in the atomic ratio 85:15) with sodium borohydride [22]. All the catalysts were 20 wt.% metal on carbon black Vulcan XC-72 (Cabot). In order to evaluate them, commercially Pt supported catalyst provided by ETEK (Natick, MA), 20 wt.% Pt supported on Vulcan XC-72, was employed.

2.1. Physical characterization of the electrocatalysts

The atomic ratios of the bimetallic PtX/C electrocatalysts were determined by energy dispersive X-ray analysis (EDX), coupled to the scanning electron microscopy LEO Mod. 440 with a silicon detector and Be window, applying 20 keV (Table 1). All the materials in the text are referenced to the nominal composition.

X-ray diffractograms (XRD) of the electrocatalysts were obtained with a universal diffractometer Carl Zeiss-Jena, URD-6, operating with Cu Kα radiation (λ = 0.15406 nm) generated at 40 kV and 20 mA. Scans were done at 3° min^{-1} for 2θ values between 20° and 100°. In order to estimate the particle size from XRD, Scherrer's equation was used [23]. For this purpose, the (2 2 0) peak of the Pt fcc structure around $2\theta = 70^\circ$ was selected. In order to improve the fitting of the peak, diffractograms for 2θ values varying from 60° to 80° were recorded at 0.02° min^{-1}. The lattice parameters were obtained by refining the unit cell dimensions by the least squares method [24].

2.2. Electrode preparation and spectroelectrochemical characterization of Pt–metal/C electrocatalysts

All experiments were carried out in electrochemical flow cells using a three-electrode assembly at room temperature. A high surface area carbon rod was used as counter electrode and a reversible hydrogen electrode (RHE) in the supporting electrolyte was employed as reference electrode. All potentials in the text are referenced to this electrode. These experiments were carried out in 0.1 M perchloric acid, prepared from high purity reagents (70% Merck p.a.) and Milli-Q water (Millipore). The electrolyte was saturated with pure argon (99.998%, Air Liquide) or CO gases (99.997%, Air Liquide), depending on the experiments.

Electrochemical studies were carried out using a HEKA potentiostat–galvanostast PG310. To characterize the quality of the electrocatalysts, cyclic voltammograms (CVs) were

Table 1
Physical properties of the carbon-supported electrocatalysts

Catalyst type	Pt ETEK[a]	PtRu [20]	PtOs [21]	PtCo [22]
Particle size (nm)[b]	3.8	2.6	4.6	3.8
Nominal composition	–	80:20	80:20	85:15
Atomic composition[c]	–	84:16	85:15	85:15

[a] Provided by E-TEK (Natick, MA).
[b] XRD.
[c] EDX.

recorded in the supporting electrolyte solution between 0.05 and 0.80 V at a scan rate of 0.02 V s^{-1}. CO stripping voltammograms were obtained after bubbling this gas in the cell for 10 min at 0.20 V, followed by electrolyte exchange and argon purging to remove the excess of CO. The admission potential was selected considering that for this value maximum adsorbate coverage is achieved for both CO and methanol at Pt. CVs were obtained in the 0.05–0.95 V potential range, starting from 0.20 V at a scan rate of 0.02 V s^{-1}.

FTIRS experiments were performed with a Bruker Vector 22 spectrometer equipped with a mercury cadmium telluride detector. A small glass flow cell with a 60° CaF_2 prism at its bottom was used. The cell and experimental arrangements have been described in detail elsewhere [25,26]. FTIR spectra were acquired from the average of 128 scans, obtained with 8 cm^{-1} resolution at selected potentials, by applying 0.05 V single potential steps from a reference potential, in the positive going direction. The reflectance ratio R/R_0 was calculated, where R and R_0 are the reflectances measured at the sample and the reference potential, respectively. In this way, positive and negative bands represent the loss and gain of species at the sampling potential, respectively.

The working electrodes consisted of a certain amount of the metal/C catalysts deposited as a thin layer over a polycrystalline gold disk. The geometric area of the disk was 0.785 cm^2. An aqueous suspension of 4.0 mg ml^{-1} of the metal/C catalyst was prepared by ultrasonically dispersing it in 15 μl of Nafion (5 wt.%, Aldrich) and pure water (Millipore). An aliquot (20 μl) of the dispersed suspension was pipetted on the top of the gold disk and dried at ambient temperature.

3. Results and discussion

Fig. 1 shows the cyclic voltammograms for the stripping of a monolayer CO formed at 0.20 V on the catalyst surface, as well as the second cycle after oxidation which corresponds to the voltammogram in the base electrolyte for the clean surface. These CVs were recorded for each material prior to the acquisition of a FTIRS series of spectra. In all cases a peak is developed during CO electrooxidation, except for $Pt_{85}Co_{15}$ where two contributions are well defined. The reason for these two peaks cannot be concluded from this simple electrochemical study, but several possibilities can be considered: the presence of two types of adsorbates, some segregation of the components of the alloy or the existence of different adsorption energies. These assumptions will be reconsidered later on the basis of the spectroscopic results.

More important than the shape of the CVs and the position of the peak potential, concerning the behaviour of the catalyst in a PEM fuel cell, is the onset for the CO oxidation to CO_2. This parameter allows the prediction of the CO poisoning of the catalyst surface at the working potential of the PEM. The onset potential is very difficult to be established from the electrochemical stripping measurements, as other processes (double layer charging and adsorption of OH prior to the formation of the oxides) occur simultaneously and contribute to the recorded current. Then, it is important to find a technique more appropriate for its determination and this could be in situ FTIRS.

A series of spectra acquired during the oxidation of a monolayer CO, with a reference spectrum obtained at 0.20 V, is given in Fig. 2. The negative band at 2343 cm^{-1} corresponds to the production of CO_2 [26] and it is apparent for $E > 0.50$ V. Other signal is observed that first appears as bipolar at 2074–2050 cm^{-1} and turns positive from 0.75 V upwards. Positive bands in the in situ FTIR spectra are related to species present at the reference but not at the sample potential. In this case, we attribute the band at 2058 cm^{-1} to linear adsorbed CO (CO_L) [26]. In the range 0.30–0.70 V the feature is bipolar because this adsorbate is still present at the surface and suffers an important wavenumber shift as a consequence of increasing the potential. A small band is also apparent at 1837 cm^{-1} which is assigned to bridge bonded CO (CO_B) [26].

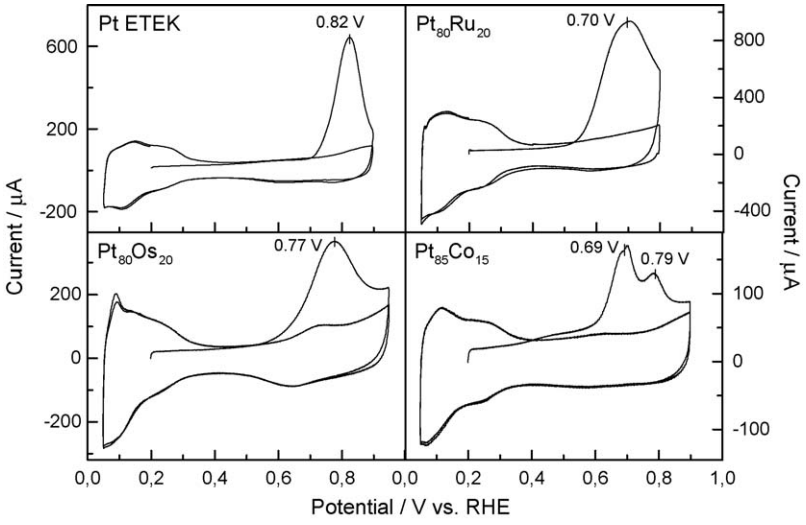

Fig. 1. CVs for the oxidative stripping of CO at Pt ETEK, $Pt_{80}Ru_{20}$, $Pt_{80}Os_{20}$ and $Pt_{85}Co_{15}$ in 0.1 M $HClO_4$. Adsorption potential = 0.20 V. After adsorption, CO was displaced from solution by electrolyte exchange and argon purging. Sweep rate = 0.02 V s^{-1}. Also the second potential scan is shown (this CV coincides with that for the clean metal in the supporting electrolyte).

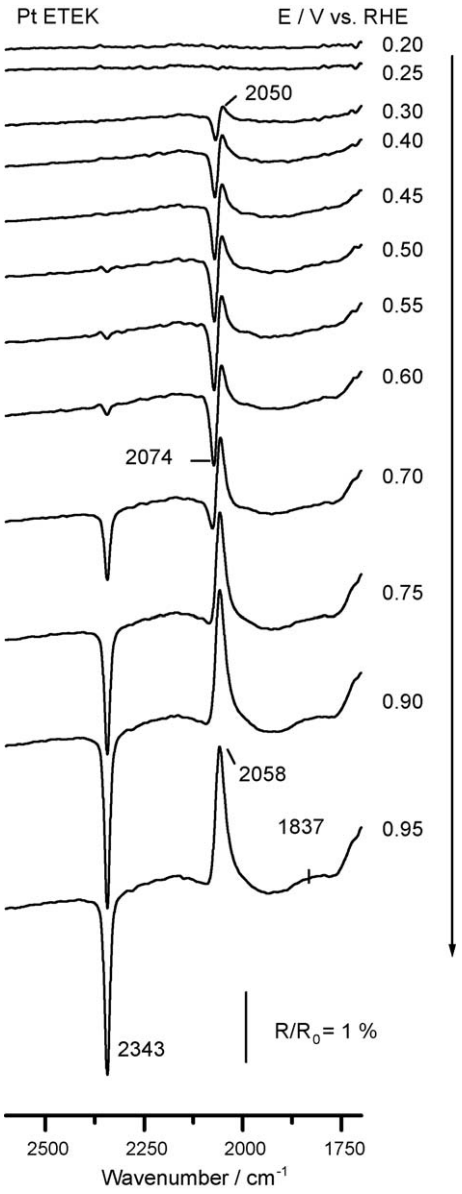

Fig. 2. In situ FTIR spectra for the oxidation of CO adsorbed on Pt ETEK in 0.1 M $HClO_4$. The CO adlayer was formed as explained in Fig. 1. The potential was positively changed from 0.20 V (reference potential) onward in 0.05 V steps up to 0.95 V. The sample potentials are indicated at the right end of the corresponding spectra.

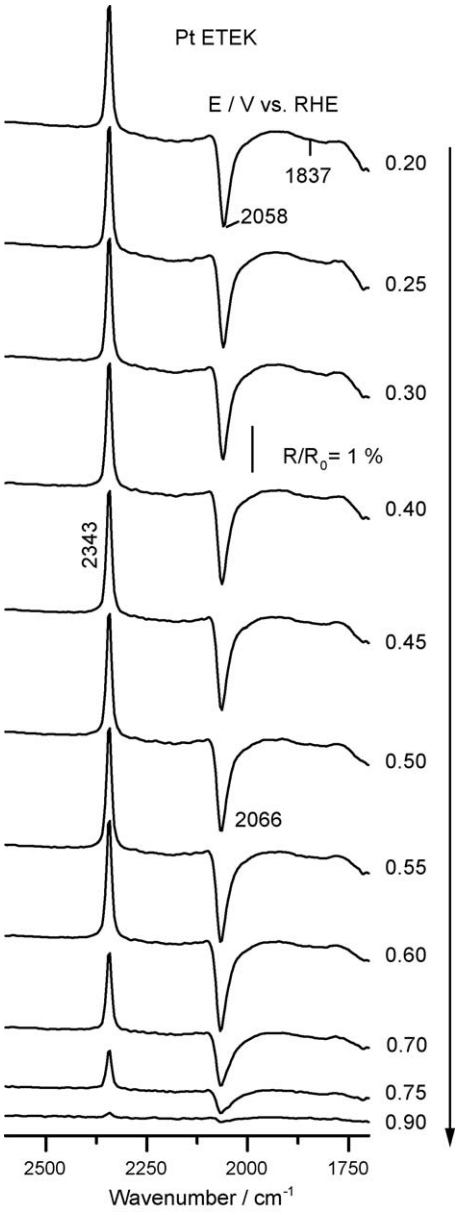

Fig. 3. Recalculated in situ FTIR spectra from Fig. 2. The reference spectrum was taken at 0.95 V, i.e. a potential where CO adsorbed was completely oxidised. The sample potentials are indicated at the right end of the corresponding spectra.

CO_2 production and CO_L oxidation can be followed integrating the corresponding bands and plotting the results as a function of the potential. In the case of carbon dioxide the integration is performed from the spectra in Fig. 2, but this is not possible for carbon monoxide as bipolar bands cannot be integrated. However, there is the possibility to obtain absolute bands changing the reference potential and choosing one where no adsorbate is present on the surface, in our case 0.95 V. In this way, spectra are recalculated as shown in Fig. 3 and the integral for CO_L evaluated. It has to be mentioned that the change in the reference implies that now the adsorbed species appears as negative bands and the CO_2 production as positive. The integrated absolute values are given in Fig. 4.

The same procedure has been followed with the bimetallic C-supported alloys and the results for the integration are also included in Fig. 4. Infrared spectra show for these electrocatalysts the same features observed for Pt, with a strong band due to CO_L and a weak one corresponding to CO_B. However, in the case of $Pt_{85}Co_{15}$, a positive feature is also developed for $E > 0.45$ V at 1244 cm^{-1}, once the oxidation to CO_2 starts (Fig. 5), with a continuous increasing in intensity up to 0.95 V. The presence of other adsorbed species could justify the second peak in the stripping voltammogram in Fig. 1. According with data in the literature, a band located approximately at this wavenumber is expected for COH [26]. It should be noticed that the hydrogen adsorption region, clearly defined in the Pt ETEK electrode below 0.40 V (see Fig. 1), is also present for the PtX

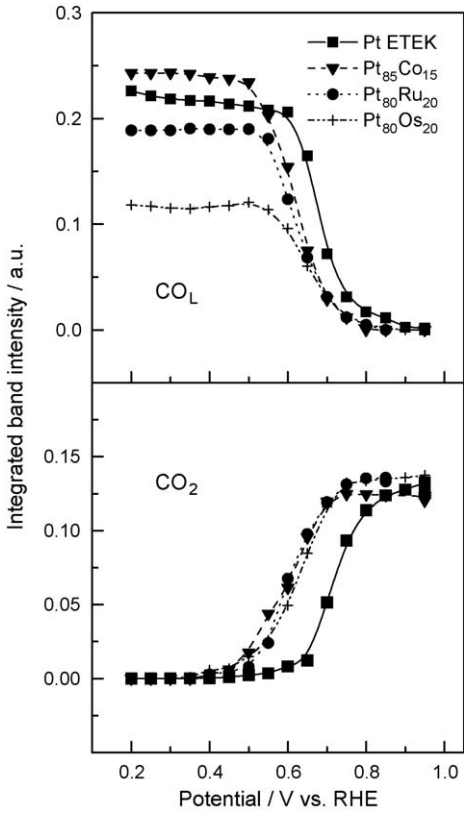

Fig. 4. Potential dependence of the integrated band intensity for CO (signal about 2050 cm^{-1}) and CO_2 (signal at 2343 cm^{-1}) obtained from CO stripping spectra on Pt ETEK, $Pt_{80}Ru_{20}$, $Pt_{80}Os_{20}$ and $Pt_{85}Co_{15}$.

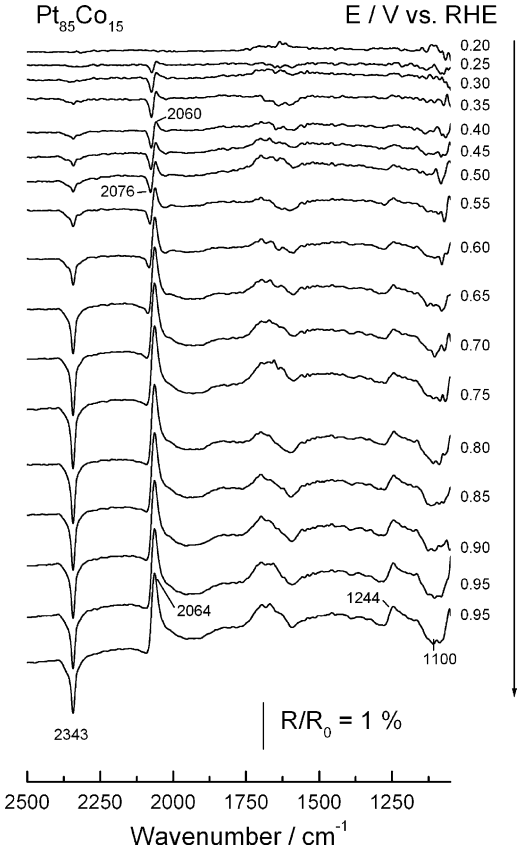

Fig. 5. In situ FTIR spectra for the oxidation of CO adsorbed on $Pt_{85}Co_{15}$ in 0.1 M $HClO_4$. The CO adlayer was formed as explained in Fig. 1. The potential was positively changed from 0.20 V (reference potential) onward in 0.05 V steps up to 0.95 V. The sample potentials are indicated at the right end of the corresponding spectra.

alloys, i.e. CO adsorption at 0.20 V occurs at surfaces partially covered with H-adatoms. Under these conditions, CO molecules can interact with adsorbed hydrogen to form COH species. A feature in this wavenumber region also appears for $Pt_{80}Os_{20}$ at $E > 0.80$ V but shows a much lower intensity.

No indication of segregation is observed in the spectra of $Pt_{85}Co_{15}$ (only one strong CO_L band is recorded) and the small intensity of the CO_B signal cannot justify the presence of a second peak in the CV (the spectra for the other catalysts also display a CO_B signal with similar intensity).

The differences in the current values observed in the CVs in Fig. 1 are also remarkable. This result is due to the different amounts of the catalysts deposited on the gold substrate. Even if the procedure of electrode preparation is carefully followed, it is impossible to reproduce exactly the amount of catalyst deposited. Accordingly, the intensity of the FTIR signals is expected to be lower if the amount of the catalysts decreases. Then, the absolute integrated values would not be comparable.

However, the integration of the CO stripping in the CVs can be used as a test reaction for the evaluation of the electrode area [1]. For all these catalysts CO is the main adsorbed species (only traces of other intermediates were detected). Then, in a first approximation, the charge involved in the stripping is due to the oxidation of CO_{ad} to CO_2 with the transfer of two electrons. As the amount of CO_{ad} is directly related to the amount of the bimetallic alloy, the charge involved in the process reflects the real electrochemical area of the electrode. Accordingly, the values for the integrated intensities in Fig. 4 are normalized with respect to the charge involved in this process (as mentioned before, CVs have been recorded just before the FTIRS measurements for the same electrode and then correspond to the same catalyst loading).

The CO_2 production curve for the Pt ETEK electrode in Fig. 4 allows the establishment of the onset potential at 0.50 V, but a fast increase is only observed at $E > 0.60$ V simultaneously with the sharp decrease in the adsorbed CO_L coverage. The onset potential for the three bimetallic C-supported electrocatalysts is shifted about 0.20 V to more negative potentials, as well as the CO_L desorption, and therefore, a better performance with respect to Pt ETEK is predictable for all of them in a polymer electrolyte membrane fuel cell (PEMFC). However, the presence of more hydrogenated residues accompanying CO_L, in our case the presence of COH, for $Pt_{80}Os_{20}$ and especially for $Pt_{85}Co_{15}$, probably enhances the poisoning of the surface when compared with $Pt_{80}Ru_{20}$. Then the latter is expected to show the best efficiency in the PEM fuel cell.

Finally, the band centre frequency shift for CO is studied as a function of the potential (Fig. 6). These values have been obtained from spectra recalculated as those in Fig. 3. The increase of the band centre with the applied potential for CO

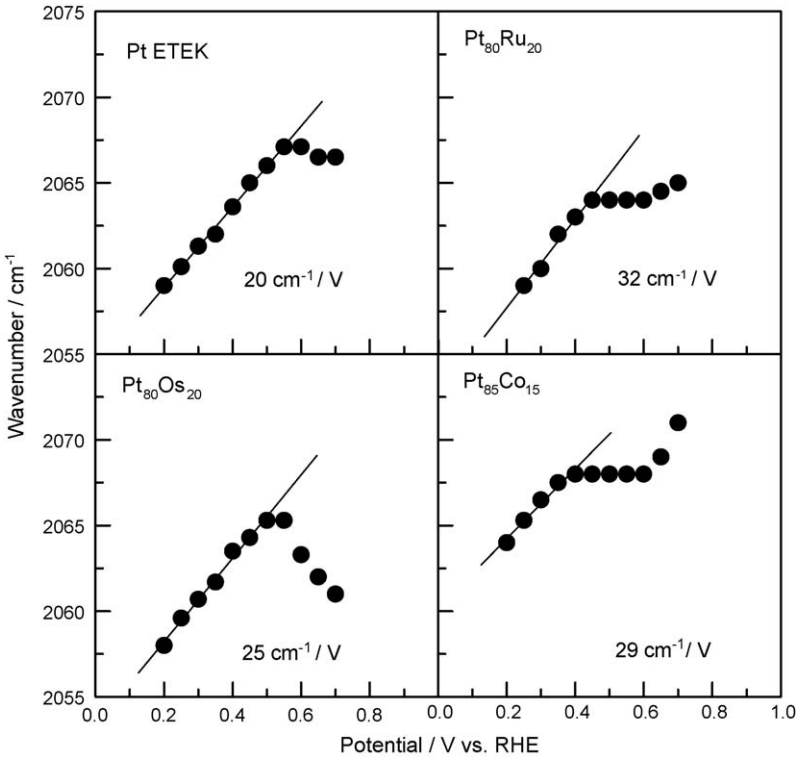

Fig. 6. Potential dependence of the band centre frequency for CO_L from CO stripping spectra on Pt ETEK, $Pt_{80}Ru_{20}$, $Pt_{80}Os_{20}$ and $Pt_{85}Co_{15}$.

vibrations can be explained on the bases of the metal–CO back-bonding or the perturbation of the vibrational frequency in the static electric field of the double layer (electrochemical Stark effect), in addition to the effect of the lateral interaction between adsorbed molecules [26,27]. A linear shift (Stark tuning) of the C–O stretch frequency with electrode potential is observed for all surfaces in the potential region before the onset of CO_L oxidation. This reflects that the electric field in the inner Helmholtz layer contributes dominantly to the shift of the C–O frequency, while CO_L coverage and binding geometry are basically constant.

Band centre values are similar for Pt, $Pt_{80}Ru_{20}$ and $Pt_{80}Os_{20}$ materials, and a blue shift is clearly visible for $Pt_{85}Co_{15}$ at the same potentials. All four materials differ in the value for the tuning rate which is then a characteristic for each system. Wavenumber values are lower for the C-supported materials than for polycrystalline Pt and PtRu electrodes, but the tuning rates are similar [27]. This fact indicates that the supported metal nanoparticle keeps the metal surface properties although the adsorption binding energies are partially affected. A more detailed analysis of this behaviour is out of the scope of the present paper, but will be the discussed in detail in a forthcoming publication.

4. Conclusions

CO adsorption and oxidation at Pt C-supported catalysts used for the anode or the cathode in PEMFCs have been studied in an electrochemical cell applying Fourier transform infrared spectroscopy. For all studied materials, the formation of linear adsorbed CO as the main residue was established, as well as the presence of small amounts of the bridge configuration. In the case of $Pt_{85}Co_{15}$ and $Pt_{80}Os_{20}$, also COH species were detected. CO stripping voltammetry allows the normalization of the surface of the electrocatalysts for a comparative analysis of the results. The shift in the onset of CO_2 production to lower potentials predicts a better efficiency of the bimetallic catalysts in the PEM fuel cell with respect to Pt ETEK. From the FTIR spectra, fundamental information can be obtained on the CO adsorption energies and metal properties of these systems, and will be the subject of future studies. A better understanding of the fuel cell reactions of bimetallic catalysts can then be achieved.

Acknowledgments

The authors thank the MEC (project MAT2002-01685 and MAT2005-06669-C03-02, FEDER) and Gobierno Autónomo de Canarias (project PI2003/070), as well as the Conselho Nacional de desenvolvimento Científico e Tecnológico (CNPq, Proc. 140205/2001-2) and the Fundação de Amparo a Pesquisado Estado de São Pulo (FAPESP, Proc. 99/06430-8 and Proc. 03/04334-9) for financial support. G.G. thanks the MCYT for FPI fellowship (BES-2003-0919). J.S.-Ch. and O.G.-V. acknowledge Cajacanarias grants at the ULL. Thanks are due to W.H. Lizcano-Valbuena, E.C. Bortholin and J.R.C. Salgado for the synthesis and characterization of the PtRu, PtOs and PtCo materials, respectively.

References

[1] W. Vielstich, A. Lamm, H.A. Gastaiger (Eds.), Handbook of Fuel Cells, Wiley, Chichester, 2003.

[2] V. Jalan, E.J.J. Taylor, J. Electrochem. Soc. 130 (1983) 2299.
[3] W.H. Lizcano-Valbuena, D. Caldas de Acevedo, E.R. Gonzalez, Electrochim. Acta 49 (2004) 1289.
[4] M.T. Paffett, G.J. Berry, S. Gottesfeld, J. Electrochem. Soc. 135 (1988) 1431.
[5] T. Toda, H. Igarashi, H. Uchida, M. Watanabe, J. Electrochem. Soc. 146 (1999) 3750.
[6] M. Watanabe, M. Uchida, S. Motoo, J. Electroanal. Chem. 229 (1987) 395.
[7] A.M. Castro Luna, G.A. Camara, V.A. Paganin, E.A. Ticianelli, E.R. González, Electrochem. Commun. 2 (2000) 222.
[8] C. Roth, N. Martz, H. Fuess, Phys. Chem. Chem. Phys. 3 (2001) 315.
[9] J.B. Goodenough, A. Hamnett, B.J. Kennedy, R. Manoharam, S.A. Weeks, Electrochim. Acta 35 (1990) 199.
[10] E.R. Gonzalez, E.A. Ticianelli, A.L.N. Pinheiro, J. Perez, Brazilian Patent, INPI-SP No. 00321 (1997).
[11] W.H. Lizcano-Valbuena, V.A. Paganin, C.A. Leite, F. Galembeck, E.R. Gonzalez, Electrochim. Acta 48 (2003) 3869.
[12] F. Colmati Jr., W.H. Lizcano-Valbuena, G.A. Camara, E.A. Ticianelli, E.R. Gonzalez, J. Braz. Chem. Soc. 13 (2002) 474.
[13] A.K. Shukla, M. Neegat, P. Bera, V. Jayaram, M.S. Hegde, J. Electroanal. Chem. 504 (2001) 111.
[14] P.A. Attwood, B.D. McNicol, R.T. Short, J. Appl. Electrochem. 10 (1980) 213.
[15] T. Frelink, W. Visscher, J.A.R. van Veen, J. Electroanal. Chem. 382 (1995) 65.
[16] A. Kabbabi, F. Gloagen, F. Andolfatto, R. Durand, J. Electroanal. Chem. 373 (1994) 251.
[17] S. Mukerjee, J. McBreen, J. Electroanal. Chem. 448 (1998) 163.
[18] O. Wolter, J. Heitbaum, J. Ber Bunsen-Ges, Phys. Chem. 88 (1984) 2.
[19] H. Baltruschat, in: A. Wiecowski (Ed.), Interfacial Electrochemistry: Theory, Experiment and Applications, Marcel Dekker, New York, 1999, p. 577.
[20] W.H. Lizcano-Valbuena, A. de Souza, V.A. Paganin, C.A.P. Leite, F. Galembeck, E.R. Gonzalez, Fuel Cells 2 (2002) 1.
[21] E. de Camargo Bortholin, Dissertacao de Maestrado, IQSC-USP, 2002.
[22] J.R.C. Salgado, E. Antolini, E.R. Gonzalez, J. Phys. Chem. B 108 (2004) 17767.
[23] B.E. Warren, X-ray Diffraction, Addison-Wesley, Reading, MA, 1969.
[24] Y.P. Mascarenhas, J.M.V. Pinheiro, Programa para Calculo de Parametro de Rede pelo Metodo de Minimos Quadrados (SBPC), 1985.
[25] T. Iwasita, F.C. Nart, in: H. Gerischer, C.W. Tobias (Eds.), Advances in Electrochemical Science and Engineering, vol. 4, VCH, New York, 1995, p. 123.
[26] T. Iwasita, V.F.C. Nart, Prog. Surf. Sci. 55 (1997) 271, and references therein.
[27] W.F. Lin, T. Iwasita, W. Vielstich, J. Phys. Chem. B 103 (1999) 3250.